

Experimental Studies of Hydroelastic Instabilities of Cavitating Hydrofoils

PAUL KAPLAN* AND AUGUST F. LEHMAN†
OCEANICS, Inc., Plainview, N. Y.

The results of water tunnel tests for determining the conditions for the occurrence of hydroelastic instabilities (flutter and/or divergence) of cavitated finite-span hydrofoils are presented. The only variable parameters in these tests were the foil density ratio and the cavity length. The tests were carried out for range of cavity lengths from one-half the chord up to twice the chord, thereby covering conditions from partial cavitation to supercavitation. No flutter or divergence was experienced in these tests for the particular parameter conditions considered, but continuous (and often severe) oscillations were experienced in all tests when the cavity length was approximately equal to 0.75 times the chord. These oscillations occurred in both degrees of freedom, were bounded in amplitude, and had constant frequency for each particular case. The oscillations were associated with fluctuations of the cavity and the resulting hydrodynamic forces. A discussion of the capability of available theory to predict the occurrence of various hydroelastic phenomena of cavitated foils is presented, together with recommended procedures for further development of theoretical techniques.

Nomenclature

a	= dimensionless distance between midchord and elastic axis, in half-chord lengths, positive when elastic axis is aft
b	= half-chord length
b_n	= coefficients in representation of complex fluid perturbation velocity; used in quasi-steady analysis
c	= foil chord length
h	= translational displacement, positive down
I_α	= mass polar moment of inertia/unit span of rotary elements about the elastic axis
j	= $(-1)^{1/2}$
K_h, K_α	= spring constants in translation and rotation, respectively
ℓ	= cavity length, measured from the foil leading edge
L	= lift/unit span
m	= total mass of foil-support system/unit span
m_h	= mass of translating parts/unit span
m_α	= mass of rotating parts/unit span
M_0	= moment/unit span, about midchord, positive for leading edge up
M_α	= moment/unit span, about elastic axis
p	= static pressure
p_v	= water vapor pressure
$\Delta p = p - p_v$	= pressure difference
r_α	= dimensionless radius of gyration of hydrofoil section about elastic axis, in half-chord lengths, $r_\alpha^2 = I_\alpha/m_b^2$
t	= time; also, foil maximum thickness
V	= freestream velocity
V_D	= divergence speed
x_α	= distance from elastic axis to center of gravity, measured in half-chords
α	= rotational displacement, positive when leading edge is up
$\beta = m_\alpha/m$	= coupling mass ratio
λ	= effective camber parameter
μ	= density ratio, $\mu = m/\rho\pi b^2$

μ_{cr}	= critical density ratio
ρ	= fluid density
σ	= cavitation number, $\sigma = \Delta p/(1/2)\rho V^2$
ω_h, ω_α	= uncoupled translational and rotational natural frequencies, respectively; $\omega_h^2 = K_h/m$, $\omega_\alpha^2 = K_\alpha/I_\alpha$
ω	= circular oscillation frequency

Introduction

THE development of high-speed hydrofoil craft requires an extensive degree of knowledge concerning the various dynamic characteristics of the hydrofoil systems under cavitating conditions. The generally accepted limit for subcavitated hydrofoil designs is considered to be in the range of speed of 50–60 knots, with higher speeds resulting in the foils being partially cavitated and, ultimately, supercavitated in the range of speeds around 100 knots. One of the important dynamic problems that face designers of these craft is the possibility of the occurrence of hydroelastic instabilities, especially flutter, at these high speeds.

At present, there exist theoretical techniques for predicting the occurrence of hydroelastic instabilities on both partially cavitated and supercavitated hydrofoils.¹⁻³ However, no experimental verification has been made of the prediction capabilities of these theories for representative operational conditions. The theoretical results in the preceding references point out the definite dangers of experiencing flutter under cavitated conditions in the range of density ratios appropriate to actual existing or contemplated foil designs. Therefore, it is considered necessary to carry out an experimental program in order to provide definite answers as to the occurrence of these instabilities, which will have a fundamental effect on the future development of high-speed hydrofoil craft.

Previous studies for the case of fully wetted flow⁴ have demonstrated a discrepancy between the theoretically predicted and experimentally measured flutter speeds at low density ratios. The theoretical prediction for this case is unconservative since the flutter speed and the critical density ratio are found by experiment to be lower than the theoretically predicted values. In view of this difficulty for a much more simple flow pattern (i.e. fully wetted flow), the experimental determination of the instability conditions for cavitated flow is of even greater concern if further progress in the development of high-speed hydrofoil craft is to be made.

The present investigation is an experimental program aimed at determining the conditions under which it is possible for

Presented at the AIAA Symposium on Structural Dynamics and Aeroelasticity, Cambridge, Mass., August 30–September 1, 1965 (no preprint number; published in bound volume of preprints of the meeting); submitted September 17, 1965. Work was supported by the Bureau of Ships, Department of the Navy, under Contract NObs-88361.

* President.

† Head, Water Tunnel Division.

finite-span hydrofoils to experience flutter under conditions of partial cavitation and also supercavitation. Comparisons with available theoretical prediction techniques are made in order to determine the reliability of predicting such dangers of hydroelastic instabilities under these operating conditions.

Experimental Investigations

The experimental portion of this investigation was undertaken in the Oceanics water tunnel. A water tunnel is an ideal tool for investigation of hydrodynamic effects under cavitating conditions, since the degree of cavitation is controllable by the tunnel operator. This tunnel is a recirculating, closed jet tunnel that is described in Ref. 5.

The test equipment consisted of three major elements: 1) the foils; 2) the elastic mounting system for the foils, enabling the foil to undergo motion in the transverse direction and rotational motion about its mounting axis; and 3) the sensing and recording instrumentation for the foil motions.

Since the experiments covered conditions wherein the cavity length would vary from about midchord of the foil to several foil lengths, certain design restrictions were imposed on the foil shape. The foil was designed such that it would be representative of a supercavitating foil shape, and the occurrence of partially cavitating flow would be associated with "transition" conditions from fully wetted to supercavitating flow. A flat plate bottom surface was chosen for simplicity in manufacture and, also, for the case of determining associated theoretical hydrodynamic characteristics for such a bottom surface (camber line for a supercavitating foil). The thickness and other shape characteristics were selected such that the cavity would be able to "close" on the rear half-chord of the foil without any interference from the upper surface ordinates. The foil cross-section had a wedge-shaped leading edge region formed by a straight surface at an angle of $7^\circ 25'$ to the flat bottom ($t/c = 0.065$), with the aft portion formed by an arc of a circle which is faired into the forward wedge portion at midchord. The foil section is shown in Fig. 1.

Two foils were fabricated, one of steel, the other of aluminum. In order to obtain the same effective mass moment of the purely rotational mass elements about the elastic axis for the two foils, a small additional weight was added to the aluminum foil by the use of an arm and weight attached to the mounting shaft. This element was not in the flowstream but was located, together with the other portions of the mounting system, on the outer side of the tunnel wall. The mounting shaft was located at the quarter-chord point, thereby resulting in an elastic axis position that would avoid divergence difficulties for both partial and supercavitating conditions. On the basis of information presented in Refs. 1 and 6, it appeared that this location would give sufficient

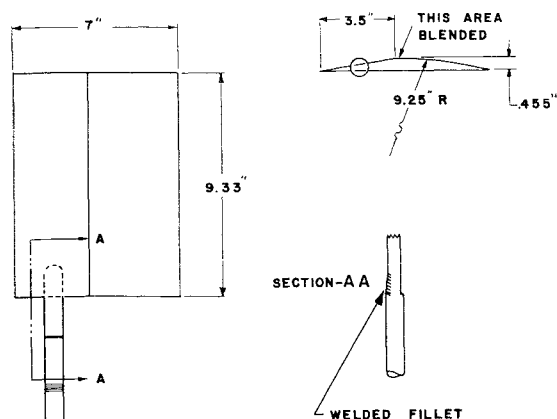


Fig. 1 Model foil section and construction details.

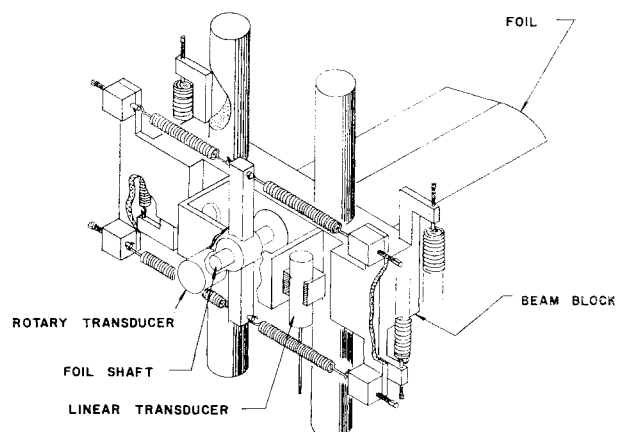


Fig. 2 Sketch of foil and elastic mounting system.

safety from divergence. The chord size was 7 in., and the foils had a span of 9.33 in.

The mounting system required an elastic support that would permit freedom in both the translational and rotational directions. In addition, because the flow velocity was to be varied, the total restraining force on the foil had to be adjustable without introducing a change in the elastic response of the system. The basic concept of the mounting system developed for this study required the foil (with an integral shaft extending from one end) to be placed in the flowing stream, so that the shaft extended through a slot in the wall of the tunnel (the wall here being a removable mounting plate). The flow, therefore, encountered a foil essentially flush with one wall while the other end of the foil was in the freestream. The shaft was captured in a bearing, so that the shaft (and foil) was free to revolve about the shaft axis. This bearing, in turn, was placed in a beam block. The beam block could move up and down transverse direction of the foil as the ends of the block (containing bearings) rode on two highly polished rods. Thus translational motions were afforded by the motion of the beam block, whereas rotational motions were afforded by the turning of the shaft in its mounting bearing.

The elastic restraint was provided by extension springs. Four extension springs were used to "hold" the beam block (and foil) in the desired transverse position. Four extension springs connected to arms extending from the foil shaft were used to hold the foil in the desired angular position. One end of each spring could be adjusted; thus the total force supplied could be readily varied, whereas the elastic spring rate remained constant. A sketch of the mounting system concept is shown in Fig. 2. The system displacements (relative to an equilibrium position) were limited to ± 0.4 in. in translation and $\pm 6^\circ$ of rotation without altering the spring characteristics.

The design requirements were such that the system had to permit the basic foil position to be changed; the springs had to have the capability of being adjusted while testing was in operation, and devices had to be incorporated for applying perturbation impulses to the foil during the test runs. Since the shaft passed through the side of the tunnel, this required the entire mechanism to operate in a water-filled box attached to the side of the tunnel. Therefore, all adjustments had to be made through the box itself. A photograph of the system mounted on the tunnel is shown in Fig. 3, whereas the same system enclosed by the box (which was filled with water during testing operations) is shown in Fig. 4.

The actual motions of the foil in both the transverse and rotational directions were recorded in order that the response of the foil to an impulse could be analyzed. The motions of the foil were sensed by linear and rotational differential

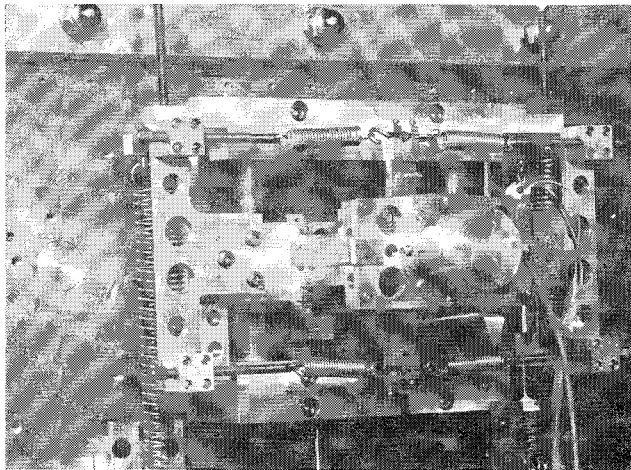


Fig. 3 Photograph showing foil-support system mounted on tunnel.

transformers, and the output from these transducers fed into an optical galvanometer recording system.

In undertaking the tests, the foil was mounted in the support system, and the natural frequencies (in air and submerged) of the foil-support system were obtained in both the transverse and rotational directions (pure uncoupled mode values). The natural frequencies for the two foils, in air and when submerged in water, are given in Table 1.

After the natural frequencies of the foil-support system were obtained, the tunnel was filled with water, and the tunnel water degassed, so that air would not come out of solution at the low test section pressures employed. When the water had been sufficiently degassed, a low absolute pressure was obtained. The velocity of the tunnel was then slightly increased. While increasing the water velocity, the foil was "locked" in the transverse direction, but its proper angular position was maintained by adjustment of the rotary springs controlling the rotary response. When the proper cavity length was obtained, the transverse support springs were adjusted until their force just held the foil in the proper translational position. At this point, the foil was being held in the required position, with the desired cavity length, by forces generated by the spring supports. The optical galvanometer recorder was started, and an impulse was applied to the foil in the transverse direction (transverse impulses were easier to apply with this particular system, and they were employed throughout the program). The response of the foil then was recorded on optical galvanometer chart paper. At least two impulses and two traces were obtained for each test condition. The absolute pressure in the tunnel then was increased, thereby requiring an increase in flow velocity to obtain the

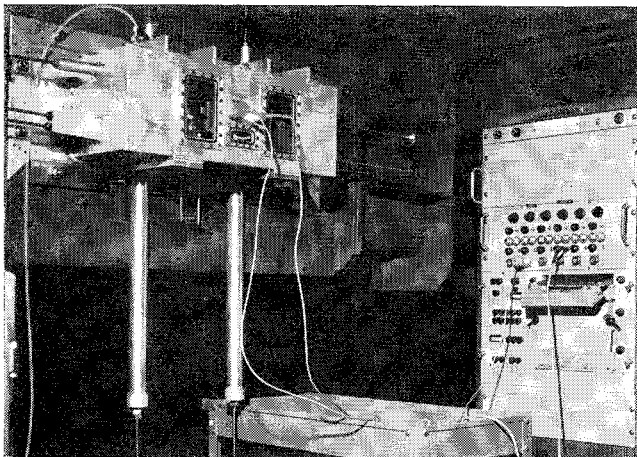


Fig. 4 Photograph showing foil-support system enclosed in box on tunnel wall.

same cavity length. When the proper conditions were reached (following the techniques previously described), the recording procedure was repeated.

The preceding test procedures were repeated for each of the desired cavity lengths until the foil-support system either exhibited undamped oscillations, or the velocity attained was so large that the restraining forces of the springs were exceeded (or the strength of the shaft support almost was exceeded). For cavity lengths in the range from 0.5 to 1.0 chords, the cavity itself becomes unstable, and severe fluctuations occur in the entire system (see Refs. 6 and 7 for instances of other occurrences of this phenomenon). Therefore, for these test conditions, the foil was locked in both the translational and rotary degrees of freedom (by means of the springs) prior to the application of the impulse.

Theoretical Analysis

The application of theoretical analysis to the problem of hydroelastic instabilities serves to predict the flutter and/or divergence conditions for particular configurations and also serves as a tool to ascertain the basic dynamic characteristics of the foil-support system in order to provide insight into the factors that influence such instabilities. Flutter and divergence boundaries can be determined from the results of Refs. 1-3 for partially cavitated and supercavitated hydrofoil systems. These conditions represent the loci of neutrally stable motions (for the flutter boundaries) where the assumed small perturbation motions are of the form $e^{j\omega t}$.

The equations of motion representing the experimental configuration are based upon a lumped-parameter system, and they are derived by means of an analysis based upon Lagrange's equations for a representative section of the system. This technique is the same as that used in Ref. 4 and leads to the same basic equations, given by

$$m\ddot{h} + m_{\alpha}\alpha\ddot{b}\ddot{\alpha} + K_{hh} = -L \quad (1)$$

and

$$I_{\alpha}\ddot{\alpha} + m_{\alpha}\alpha\ddot{b}\ddot{h} + K_{\alpha\alpha} = M_{\alpha} \quad (2)$$

where

m_{α} = mass of rotating parts/unit span

m_h = mass of translating parts/unit span

$m = m_{\alpha} + m_h$ = total mass/unit span

I_{α} = polar mass moment of inertia of rotating parts about elastic axis/unit span

All other symbols refer to quantities ordinarily occurring in hydroelastic analyses, and they are defined in the Nomenclature. The dynamic system is pictorially represented in Fig. 5.

The hydrodynamic lift and moment representations for the case of purely oscillatory perturbations (necessary for the basic flutter analysis) are given,¹⁻³ but no representation for the case of arbitrary motions is presently available. A quasi-steady hydrodynamic theory (two-dimensional flow) for oscillatory motion is available,³ and this can be adapted

Table 1 Natural frequencies of foil systems

Foil	Air, (rad/sec)	Water, (rad/sec)
Steel Foil		
Translation, ω_h	19.64	...
Rotation, ω_{α}	69.81	50.27
Aluminum Foil		
Translation, ω_h	22.44	16.12
Rotation, ω_{α}	76.16	44.88

^a No value was obtained because of the lack of a sufficient number of oscillations in this case.

readily to the present application for the case of partially cavitated foils. The main feature of quasi-steady theory is the assumption that the hydrodynamic forces acting on a hydrofoil with time-varying linear and angular velocities are equal, at any instant of time, to the forces on the same foil when it is moving with constant linear and angular velocities equal to the actual instantaneous values. In addition, within the context of understanding of the present use of quasi-steady theory, added mass contributions to the forces and moments also are included. The wake effects, which are essential for unsteady flow theory, are neglected. The quasi-steady theory is of interest here since the results are in simple form, and the conclusions, in regard to significant flutter limit conditions, are equivalent to those obtained using the more complete, unsteady hydrodynamic forces (see Ref. 3 for a discussion of the relations between both approaches to the partial cavitation flutter case).

Attempts were made to carry out an extension of the analysis of Ref. 3 to the case of supercavitating flow ($l/c > 1$), but this extension was unsuccessful. The probable cause of this inability to extend the quasi-steady theory was the neglect of wake effects (which was a valid procedure for the case of partially cavitated foils). If the cavity boundaries for a supercavitated two-dimensional foil are viewed as vortex sheets, their extension to a length greater than the foil chord requires an inclusion of wake effects in the resulting analysis. This would not allow the simple formulas of Ref. 3 to apply alone but would require a modification of those results together with additional terms for a complete representation of the quasi-steady hydrodynamic force and moment acting on a supercavitated hydrofoil. The effort required for such an analysis exceeded the scope of work required for the present study, and consideration of this aspect was deleted from the program after a preliminary analysis demonstrated the nature of the required effort.

The quasi-steady lift and moment, for the case of partially cavitated flow (Ref. 3), are given by

$$L_0 = \rho b V^2 [-2\pi b_1 + (2\pi b/V)(db_2/dt)] \quad (3)$$

$$M_0 = \rho b^2 V^2 \left[-2\pi b_2 + \frac{\pi b}{V} \frac{d}{dt} \left(b_3 - \frac{b_1}{2} \right) \right] \quad (4)$$

where M_0 is the moment about the midchord; the rotational motion also is about the midchord; and the quantities b_n are known functions

$$b_n = b_n[\alpha + \dot{h}/V, (\dot{\alpha}b/2V)]$$

For motion about the elastic axis, the moment is transferred by

$$M_a = M_0 + abL \quad (5)$$

after the replacement of the translatory motion variable h by $h - ba\alpha$, where a = dimensionless distance between midchord and elastic axis, in half-chord lengths, positive when elastic axis is aft. The quantities b_1 , b_2 and b_3 are given by

$$b_n = [\alpha + \dot{h}/V - (ba\dot{\alpha})/V](\partial b_n/\partial \alpha) + (b\dot{\alpha}/2V)(\partial b_n/\partial \lambda) \quad (6)$$

$$n = 1, 2, 3$$

where the derivative terms $(\partial b_n/\partial \alpha)$ and $(\partial b_n/\partial \lambda)$ are constants appropriate to the particular cavity length, which are evaluated numerically in Ref. 3. The lift and moment (about the elastic axis) appropriate to motion about the elastic axis are simply determined by the preceding procedures and inserted into Eqs. (1) and (2), leading to a set of coupled linear differential equations. Assuming oscillatory motion, the equations have a solution if a certain determinant is set equal to zero, yielding the flutter stability boundaries in the form of reduced velocity $V/(b\omega_\alpha)$ plotted against the density ratio $\mu = m/(\rho\pi b^2)$.

The flutter analysis for the case of supercavitated (at $\sigma = 0$) and partially cavitated foils is outlined in detail.¹⁻³ Since

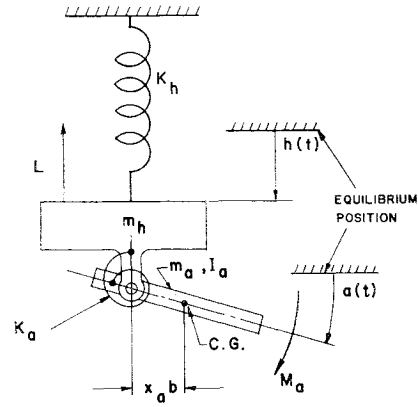


Fig. 5 Schematic diagram of system used for dynamic analysis.

the experiments in this study were limited to two values of density ratio (corresponding to the steel and aluminum foil models) without the effect of additional weights, a significant theoretical result for purposes of comparing with experiment would be the value of the critical density ratio for each of the configurations tested. The critical density ratio is the value of μ for which the flutter speed curve asymptotically approaches infinity, and it may be viewed (in the present case of unswept foils) as the lowest value of the density ratio at which flutter will occur. The result for the case of partially cavitated foils, as derived from the quasi-steady analysis of Ref. 3, is given by

$$\mu_{cr} = \frac{(\partial b_1/\partial \alpha)(\partial b_2/\partial \lambda) - (\partial b_1/\partial \lambda)(\partial b_2/\partial \alpha)}{(a + \beta x_a)(\partial b_1/\partial \alpha) - (\partial b_2/\partial \alpha)} \quad (7)$$

where the numerical values of the partial derivative terms are listed in Ref. 3. The one difference between the result given in Eq. (7) and that of Ref. 3 is the appearance of the term βx_a instead of x_a alone, because of the basic coupling in the present experimental system [Eqs. (1) and (2)] where $\beta = (m_\alpha)/m$ is the coupling mass ratio. This result is valid only for the case where $(\omega_h/\omega_\alpha) = 0$, which is not satisfied in the present experimental system. However, it is expected that Eq. (7) will give a sufficiently useful indication of the location of the critical density ratio appropriate to the needs of this study.

For supercavitated foils, the basic result of Ref. 1 can be carried over to the present configuration, resulting in a value of the critical density ratio given by

$$\mu_{cr} = \frac{\frac{2.5}{1.28}}{(a + \beta x_a) + \frac{3}{8}} \quad (8)$$

This result is derived in Ref. 1 on the basis of $(\omega_h/\omega_\alpha) = 0$, and, also for the case wherein $\sigma = 0$, i.e., for an infinite cavity length. There is no proven method of deriving an expression for the critical density ratio valid for $\sigma \neq 0$ from the results of Ref. 1 and, as discussed previously, no success was obtained in extending the quasi-steady analysis of Ref. 3 to the case of supercavitated flow with finite cavity length. Therefore, the result given in Eq. (8) is the only tool presently available for predicting the critical density ratio for supercavitated hydrofoils.

With regard to divergence, simple expressions exist for determining the critical divergence speed of partially cavitated and supercavitated hydrofoils in the results of Refs. 1 and 3. For a supercavitated hydrofoil, the divergence speed is given by

$$\frac{V_D}{(b\omega_\alpha)} = \left[\frac{2\mu r_\alpha^2}{(1 + \sigma)(a + \frac{3}{8})} \right]^{1/2} \quad (9)$$

and for the case of partially cavitated flow, the divergence

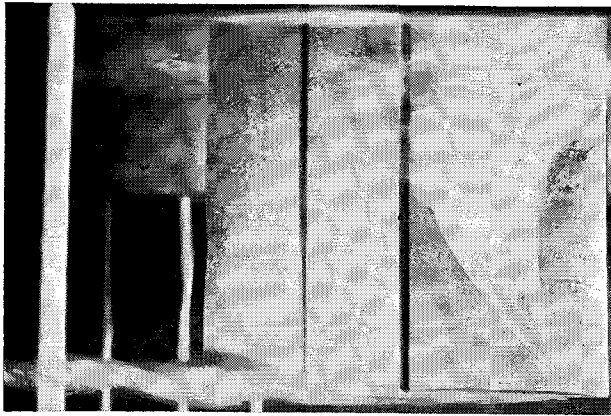


Fig. 6 Vertical view of foil and cavity for condition $l/c = 0.50$.

speed is given by

$$\frac{V_D}{b\omega_\alpha} = \frac{r_\alpha(\mu/2)^{1/2}}{[a(\partial b_1/\partial \alpha) - (\partial b_2/\partial \alpha)]^{1/2}} \quad (10)$$

Equation (9) is derived on the basis of a modification of the result for the case of an infinite cavity length ($\sigma = 0$), and its validity is questionable; but since this is the only information currently available, it should be used as a means of predicting the divergence speed for supercavitating foils.

Comparisons of the theoretical predictions with experimental results obtained in this study will be presented in a later section of this paper.

Experimental Results

The tests were carried out on the two different foil models, one made of steel and the other of aluminum. The support system was constructed of aluminum, and its mass, inertia, etc. had to be considered in evaluating the basic inertial characteristics of the entire foil support system. The basic inertial characteristics for the steel foil were as follows:

$$\begin{aligned} \mu &= 0.95 & x_\alpha &= 0.486 & \beta &= 0.497 \\ \beta x_\alpha &= 0.242 & r_\alpha &= 0.665 \end{aligned}$$

For the aluminum foil, the basic inertial characteristics are given by:

$$\mu = 0.77 \quad r_\alpha = 0.777$$

In order to attain an equivalent rotary mass moment for both foil configurations, an additional small mass was placed at a small distance from the elastic axis for the aluminum foil configuration, such that the resultant value of $\beta x_\alpha = 0.242$. With regard to other related basic dynamic characteristics of both systems, the ratio of the natural frequencies in transla-



Fig. 7 Side view of foil and cavity for condition $l/c = 0.50$.

tion and rotation was approximately equal for both cases, i.e.

$$(\omega_h/\omega_\alpha)^2 = 0.08$$

The location of the elastic axis at the foil quarter-chord point resulted in the quantity $a = -0.50$.

The cavity length conditions considered in this study range from $l/c = 0.50 - 2.0$, with particular tests at $l/c = 0.50, 0.75, 1.0, 1.25, 1.5$, and 2.0 . Following this basic series of cavity length conditions, tests also were performed for conditions where $l/c = 0.625$ and 0.875 , in order to obtain further data in a region of interest. The desired cavity length was obtained by a combination of conditions involving the static pressure in the tunnel, the forward speed, and the foil angle of attack. The angle of attack in these tests ranged from 4.5° to 18.5° , with the larger angles being associated with the largest cavity length and the lowest speeds. The range of values of the cavitation index σ (referred to vapor pressure) extended from 1.35 down to 0.44 , with the smallest value associated with the largest cavity length.

In formulating the test program, it was expected that the cavity length would be a simple function of the angle of attack and cavitation index for conditions of both partial cavitation and supercavitation, in accordance with the theoretical results given in the work of Geurst.^{8,9} This behavior was indicated as proper for the case of two-dimensional flow, but in the present case of finite-span hydrofoils, the relations would differ somewhat from those theoretical results. In addition, the flat plate bottom is the effective camber line for the case of a supercavitating hydrofoil, whereas the particular section tested actually had an effective camber line that was not a flat plate in the case of partially cavitating flow (since the mean line of the section is the effective camber line for the case of partially cavitating flow, as in fully wetted flow^{8,9}). On this basis, the same cavity length could not be obtained for a fixed value of σ by retaining the angle of attack constant. This factor increased the testing effort since it required a "searching" for proper conditions, and it did not allow universality in the conditions associated with a particular cavity length.

Illustrations of the cavity appearance, from both a vertical and side view, are shown in Figs. 6 and 7, which are, for the case of a cavity length, equal to one-half of the chord length. It can be seen that the cavity starts at the leading edge of the foil, and that its outer boundary is swept inboard, with a sharp delineation between the cavity and the surrounding wetted flow. The long trailing tip vortex sweeps straight downstream, starting from the leading edge tip of the foil in a conical form. The resulting shape and form of the tip vortex appears to be independent of the cavity on the foil upper surface. These observed characteristics of the cavity

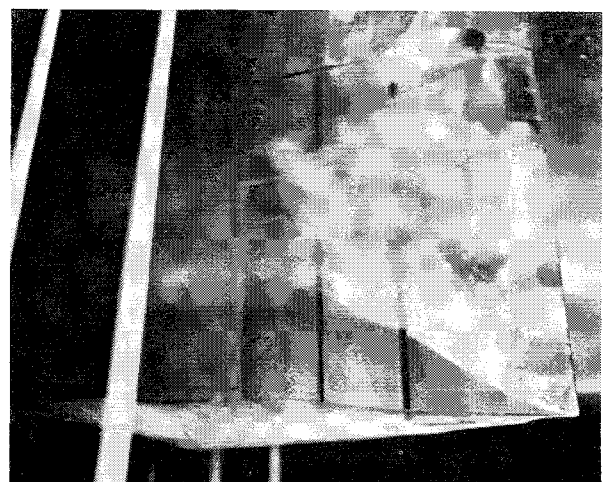


Fig. 8 Vertical view of foil and cavity for condition $l/c = 0.75$.

are in agreement with those reported in Ref. 10, thereby verifying the applicability of the present flow conditions as representative of realistic three-dimensional cavity flow patterns. The cavity length is determined visually by averaging over the rear extent of the cavity, including the "froth" portion and any re-entrant jet flow that may be associated with the particular cavity configuration. Markings were placed on the foil and within the tunnel to assist in determination of the cavity length by these visual techniques. Further illustrations of the cavity conditions obtained in the test are shown in Figs. 8 and 9, which represent a view of the upper surface of the foil when the cavity length is equal to 0.75 of the chord length, and a side view of a long cavity for the case where the cavity length is about twice the chord. The clear vapor appearance for the long cavity is very evident, whereas there is a significant amount of froth and some indication of re-entrant flow for the case of the partial cavity. Other photographs, not shown within this paper, indicate a more significant amount of re-entrant jet flow for the case where the cavity length was equal to the chord length, and when it was slightly larger than the chord.

The tests were carried out in the manner described previously. The speed range throughout the tests was from 13 through 26 fps. For partial cavitation conditions with the cavity length equal to one-half the chord, and for the supercavitated range where the cavity length was greater than 1.25 times the chord, no flutter conditions were encountered for either foil configuration. The motions were rapidly damped with the system returning to equilibrium with hardly any disturbance motion persisting. The response rate in these cases was quite rapid, and even with the use of a high-frequency optical galvanometer recording system, there was no indication of significant overshoot, oscillations, etc., in the early time instances for such stable conditions. However, there were some continuous erratic oscillations of small amplitude for some of these conditions, primarily, for the case where the cavity length was equal to 1.25 times the chord length. The erratic traces always appeared to occur mainly in the translatory degree of freedom. These motions were not of significant nature, and they are, in the main, due to the general nature of fluctuations associated with a cavity (which is never really steady) as well as the sensitivity of the recording system.

Significant oscillations did occur for the case where the cavity length-chord ratio was equal to 0.75, which is also a condition wherein previous studies have shown the cavity itself to oscillate.^{6,7} These oscillations were present in both degrees of freedom, i.e., translation and rotation, with definite values of the oscillatory period evident in the records. An example of a sample record is given in Fig. 10, which illustrates the resulting oscillation following an initial translation

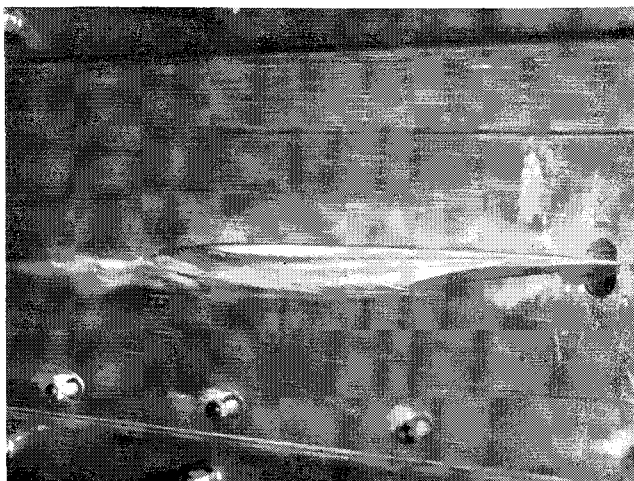


Fig. 9 Side view of foil and cavity for large cavity length condition $l/c \approx 2.0$.

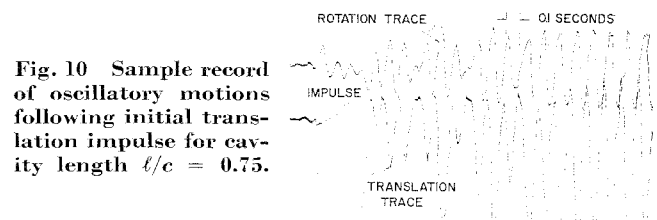


Fig. 10 Sample record of oscillatory motions following initial translation impulse for cavity length $l/c = 0.75$.

impulse to the system. The oscillations appeared to be of almost constant amplitude in each of the cases that occurred for this cavity length for both foils, and, hence, they are not to be classed as flutter phenomena. During many instances wherein such oscillations occurred, the entire tunnel also was set into vibration, and a significant amount of audible noise was evident. The records obtained under these conditions were analyzed, and it appeared that for a fixed angle of attack for each foil, the reduced frequency of oscillation was almost constant over the speed range tested. An illustration of these results is given in Fig. 11 for the case where $l/c = 0.75$, with an angle of attack of 6° for the steel foil and 9° for the aluminum foil. The angles of attack differ for the information presented in Fig. 11, since lower speeds (and hence larger angles of attack) were used in the case of the aluminum foil because of the strength limitation of that particular material. The average cavitation indices associated with these conditions also are shown on Fig. 11, and they are $\sigma = 0.76$ for the steel foil (6° angle of attack) and 0.95 for the aluminum foil (9° angle of attack). This approximately constant reduced frequency for the present test results, wherein an elastic restraint is imposed externally on the foil, is similar to the results obtained for the basic fluctuations of lift force obtained in the two-dimensional force measurement investigation of Ref. 7.

For the case where the cavity length was equal to the chord, no definite oscillation occurred in the response of the system to imposed disturbances. However, the records appear to be quite erratic, indicating persistent random fluctuations in both rotational and translational motions. This is probably because of the nature of the fluctuations associated with the cavity conditions for this particular cavity length. The occurrence of the oscillations for conditions where $l/c = 0.75$ led to further studies for the conditions wherein $l/c = 0.625$ and 0.875 (approximately attained in the experiments) in order to see if the oscillatory behavior was present for those cavity lengths. Tests at these cavity lengths were carried out only for the steel foil since the phenomena would be expected to occur for the aluminum foil as well. The test results indicated the occurrence of

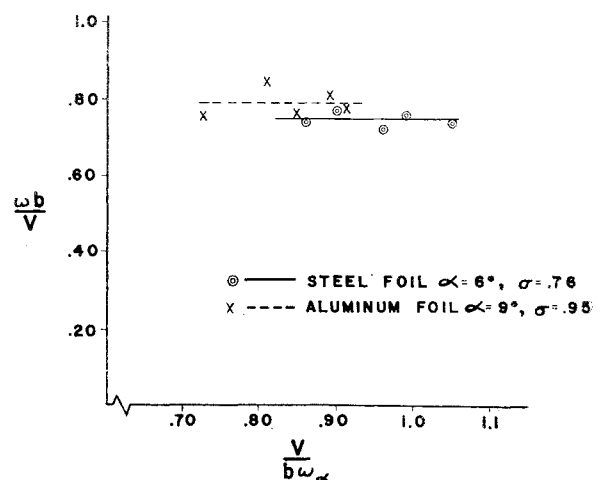


Fig. 11 Reduced frequency of oscillations as a function of forward speed for condition $l/c = 0.75$.

similar oscillations when the $l/c = 0.625$, with clearly indicated oscillations in the records. These results were not obtained for conditions with $l/c = 0.875$ where the oscillations were primarily erratic in nature, except for the higher speed conditions where discernible oscillations did occur.

The behavior exhibited in these experimental studies does not appear to be an example of a classical flutter, which was the subject of the analytical and experimental studies of Refs. 1-4. Most of the cases tested were stable configurations in the sense of the terms as used in flutter studies. The occurrence of oscillations for the conditions where the cavity length was in the neighborhood of 0.75 times the chord may be considered a limit cycle type of motion, with almost constant amplitude for each run and with an approximately constant reduced frequency over the speed range for a fixed angle of attack. This behavior is associated with conditions where other studies have shown the cavity itself to have large fluctuations that result in significant variations of the hydrodynamic force acting on the foil under these conditions. These force fluctuations are associated with variations of the cavity size and with vortices shed into the wake (Ref. 7). It was unfortunate that motion pictures of the foil oscillations and the cavity behavior were not made during these tests since such data would provide valuable insight into the nature of the oscillatory phenomena.

There is a basic question as to how to describe the observed oscillatory behavior, i.e., whether the phenomenon is one of ordinary resonance or whether it is a type of self-excitation. The resonance concept receives support from the fact that when the cavity oscillates for the stationary foil, the hydrodynamic forces also oscillate, and this leads to a periodic driving force that results in appreciable motion at the system natural frequency. An important point in this situation is the value of the frequency of the cavity and force oscillations, and how that frequency is related to the dynamic system natural frequency (which will vary with forward speed because of the presence of speed-dependent restoring moments and also coupling between degrees of freedom). The hypothesis of self-excited oscillations assumes that the effect of the oscillatory motion of the system will influence the nature of the cavity and force fluctuations, thereby acting in the capacity of a feedback system. On this basis, the oscillations could occur at the dynamic system natural frequency since the major effect of the motions will be the influence on velocity-type (damping) terms. These basic questions as to the nature of the oscillation phenomena cannot be answered at the present time because of the lack of knowledge concerning unsteady cavitation phenomena and the forces associated with such flow conditions. Similar situations still exist for the case of oscillations of cylinders and bluff bodies in fully wetted flow due to vortex shedding, and, therefore, a greater effort is necessary to obtain more knowledge of the fundamental properties of unsteady hydrodynamics for explaining vibratory phenomena of bodies in both cavitating and noncavitating flows.

Comparison of Theory and Experiment

The response characteristics of cavitating hydrofoil systems (which are elastically supported) following arbitrary impulsive perturbations have been described in detail in preceding sections. No flutter or divergence was found to occur for the particular conditions tested, but definite bounded oscillations occurred for a particular range of cavity conditions. The conditions that were similar in all cases tested were the location of the elastic axis, the value of effective static unbalance, and the ratio of the natural frequencies in translation and rotation. The actual natural frequencies (in air) were fairly close for both the steel and aluminum foil configurations (Table 1), whereas there were differences in the radius of gyration and the density ratio for the two systems. Since the values of radius of gyration were not too different, and

since this physical parameter has only a relatively small effect on flutter boundaries,^{1,2} the major difference between the two configurations was the density ratio. Although the density ratios only differed by a small amount, the relative magnitudes are significant because of the major importance of the density ratio in determining the occurrence of flutter. The effect of the variation of the cavity length is exhibited directly in these tests since all other parameters are constant for a particular density ratio value.

With regard to the effect of variation of cavity length in this program, there does not appear to be sufficient theoretical information available for purposes of comparison with experimental results. The theory for supercavitating foils is valid only for an infinite cavity length ($\sigma = 0$), and, hence, no influence of cavity length variation is discernible from that theory. For partially cavitating flow, the available theory is not applicable to conditions where $l/c > 0.75$ because of the occurrence of infinite values of the hydrodynamic variables and the multivalued nature of cavity parameters (Refs. 2 and 3). Thus, a limited set of experimental conditions hopefully can be compared with theoretical predictions in order to check the utility of available theories.

No divergence occurred for any of the configurations tested, and this may be ascribed to the location of the elastic axis ($a = -0.50$), which was selected close to the foil center of pressure to avoid divergence. With regard to flutter, the critical density ratio is the major theoretical parameter of value for carrying out any comparisons in the present investigation. In supercavitating flow ($\sigma = 0$), the value of the critical density ratio, according to Eq. (8), is found to be $\mu_{cr} = 1.47$ for the physical parameters in the present investigation. Computations for the case of partially cavitating flow, using Eq. (7), resulted in a value of $\mu_{cr} = 2.85$ for $l/c = 0.50$; whereas a negative critical density ratio value was indicated for the case where $l/c = 0.625$, leading to the conclusion that flutter is theoretically impossible at any density ratio for that particular cavity length ($l/c = 0.625$). Since the density ratios tested in the present program were $\mu = 0.77$ and 0.95 , they lie below the values of critical density ratio predicted by theory for either partially cavitating or supercavitating flow. Hence, flutter is predicted not to occur for these configurations, and there is agreement because of the nonoccurrence of flutter. This type of agreement does not instill any faith in the validity of prediction using the theoretical expressions given in Eqs. (7) and (8). Further testing with larger values of the density ratio, modifications to the system mass, center of gravity positions, elastic axis location, etc., would yield conditions for which flutter would be expected to occur. Although such alterations would cause the system to depart further from real foil designs, it would be a useful testing tool for determining the capability of theoretical prediction, as well as for illustrating the basic phenomena of flutter of cavitating hydrofoils.

The occurrence of bounded oscillations for cavity length conditions near $l/c = 0.75$ for the two foil configurations is a situation that is not amenable to comparison with available theory at the present time. Indications of the existence of some type of critical condition associated with this cavity length were available from various theoretical and experimental studies concerned with hydrodynamic force investigations. However, no complete hydrodynamic theory presently considers the flow pattern associated with the fluctuating cavity (independent of foil oscillations) that occurs in this case; and that appears to be a major unknown factor that influences the hydroelastic phenomena observed and reported in this study. It is important that a basic hydrodynamic theory be developed to account for this flowfield behavior and that further experiments involving force measurements, cavity pictures, etc., for this case be continued, following the initial studies of Ref. 7. This basic hydrodynamic data possibly will provide insight such that the oscillations associated with this cavity length condition

may be mitigated by proper choice of elastic support axis, center of gravity, etc.

The occurrence of partial cavitation of this extent is not only associated with hydrofoils at high speed, but is evident on ship rudders in high-speed operation as well (see Ref. 11 for illustrations). The oscillations demonstrated in this study might have been the causative agent of the ship vibration problem described in Ref. 12, which was the center of a great deal of scientific controversy (discussion section, Ref. 12). The possibility of this type of vibration excitation of a surface ship, as well as the recognized importance of this problem for hydrofoil development, makes this phenomenon more significant in this era of ever-increasing speed of surface craft.

Conclusions

The results of this study of hydroelasticity demonstrated the nonoccurrence of flutter and divergence for the two basic configurations tested. Available theoretical results also predicted this lack of flutter and divergence, but this is not a proper test of the prediction capabilities of the theories. Further tests over a large range of density ratio by adding weights, shifting the elastic axis position, etc., are recommended. These new tests would encompass the critical conditions that could lead to flutter and provide a check on prediction capabilities of available theories.

Although flutter did not occur, steady bounded oscillations of both foil systems occurred for conditions where the cavity length was near 0.75 times the chord. These persistent oscillations were associated with fluctuations of the cavity and the resulting hydrodynamic forces, and there are basic questions as to whether the phenomena can be classified as caused by resonance or as a self-excited oscillation. No theoretical results are presently available to aid in analyzing and/or predicting the characteristics of these oscillations. Determination of the basic hydrodynamics of unsteady flow for finite length cavities, both supercavitated and partially cavitated, is necessary for a more complete understanding of the flow characteristics that could lead to oscillations and instability of hydrofoils with elastic supports. In particular, an effort should be made to account for the fluctuation char-

acteristics of the partial cavity condition $l/c = 0.75$ in order to provide insight into means for reducing the severity of the system oscillations associated with that condition.

References

- ¹ Kaplan, P. and Henry, C. J., "A study of the hydroelastic instabilities of supercavitating hydrofoils," *J. Ship Res.* **4**, 28-38 (December 1960).
- ² Kaplan, P., "Hydroelastic instabilities of partially cavitating hydrofoils," *Proceedings of the Fourth Symposium on Naval Hydrodynamics* (Office of Naval Research, August 1962), ACR-92, pp. 775-805.
- ³ Kaplan, P. and Zeckendorf, L. J., "A study of hydroelastic stability of partially cavitating hydrofoils by application of quasi-steady theory," *Oceanics, Inc. Rept.* 64-10 (February 1964).
- ⁴ Henry, C. J., "Hydrofoil flutter phenomenon and air-foil flutter theory," Davidson Lab., Stevens Institute of Technology, Rept. 856, Vol. I (September 1951).
- ⁵ Lehman, A. F., "Some cavitation observation techniques for water tunnels and a description of the oceanics tunnel," *ASME Symposium on Cavitation Research Facilities and Techniques* (American Society of Mechanical Engineers, New York, May 1964), pp. 29-35.
- ⁶ Meyer, M. C., "Some experiments on partly cavitating hydrofoils," *Intern. Shipbuilding Progr.* **6**, 361-368 (August 1959).
- ⁷ Wade, R. B., "Water tunnel observations on the flow past a plano-convex hydrofoil," California Institute of Technology, Div. of Engineering and Applied Science, Rept. E-79-6 (February 1964).
- ⁸ Geurst, J. A., "Linearized theory for partially cavitating hydrofoils," *Intern. Shipbuilding Progr.* **6**, 369-384 (August 1959).
- ⁹ Geurst, J. A., "Linearized theory for fully cavitating hydrofoils," *Intern. Shipbuilding Progr.* **7**, 17-27 (January 1960).
- ¹⁰ Kermeen, R. W., "Experimental investigations of three-dimensional effects on cavitating hydrofoils," California Institute of Technology, Engineering Div., Rept. 47-14 (September 1960).
- ¹¹ Macovsky, M. S., Duerr, R. J., and Jewell, D. A., "An investigation of flow-excited vibration of the USS Forrest Sherman (DD931)," David Taylor Model Basin Rept. 1188 (August 1958).
- ¹² McGoldrick, R. T., "Rudder-excited hull vibration on USS Forrest Sherman (DD931) . . . (a problem in hydroelasticity)," *Trans. Soc. Naval Architects Marine Engr.* **67**, 341-385 (1959).